NASA Contractor Report 187055

The Effect of Steady Aerodynamic Loading on the Flutter Stability of Turbomachinery Blading

Todd E. Smith

Sverdrup Technology, Inc.
Lewis Research Center Group
Brook Park, Ohio

and

Jaikrishnan R. Kadambi

Case Western Reserve University
Cleveland, Ohio

December 1990

Prepared for
Lewis Research Center
Under Contract NAS3-25266

National Aeronautics and
Space Administration

THE EFFECT OF STEADY AERODYNAMIC LOADING ON THE FLUTTER STABILITY OF TURBOMACHINERY BLADING

Todd E. Smith
Sverdrup Technology, Inc.
Lewis Research Center Group
Brook Park, Ohio 44142

and

Jaikrishnan R. Kadambi
Department of Mechanical and Aerospace Engineering
Case Western Reserve University
Cleveland, Ohio 44106

ABSTRACT

An aeroelastic analysis is presented which accounts for the effect of steady aerodynamic loading on the aeroelastic stability of a cascade of compressor blades. The aeroelastic model is a two degree-of-freedom model having bending and torsional displace-ments. A linearized unsteady potential flow theory is used to determine the unsteady aerodynamic response coefficients for the aeroelastic analysis. The steady aerodynamic loading was caused by the addition of (1) airfoil thickness and camber and (2) steady flow incidence. The importance of steady loading on the airfoil unsteady pressure distribution is demonstrated. Additionally, the effect of the steady loading on the tuned flutter behavior and flutter boundaries indicates that neglecting either airfoil thickness, camber or incidence could result in nonconservative estimates of flutter behavior.

NOMENCLATURE

a	fluid sonic velocity
b	blade semichord length
$\bar{C}_p = \frac{\bar{P} - \bar{P}_\infty}{\frac{1}{2}\rho W^2}$	steady static pressure coefficient
$\Delta\tilde{C}_p = \frac{\tilde{P}}{\frac{1}{2}\rho W^2}$	unsteady pressure coefficient
$c = 2b$	blade chord length
h	chordwise normal bending displacement
$I = mr_G^2 b^2$	blade section moment of inertia abo elastic axis
i	fluid steady flow incidence angle, deg, also $\sqrt{-1}$
K_h	spring stiffness for bending
K_α	spring stiffness for torsion
$k = \frac{\omega b}{W}$	reduced frequency based on semichord
L	unsteady aerodynamic lift force per unit span
L_h	unsteady aerodynamic lift coefficient due to blade bending motion
L_α	unsteady aerodynamic lift coefficient due to blade torsional motion
M	unsteady aerodynamic moment per unit span about elastic axis
M_h	unsteady aerodynamic moment coefficient due to blade bending motion
M_R	fluid inlet relative Mach number
M_α	unsteady aerodynamic moment coefficient due to torsional motion
m	blade mass per unit span
N	number of blades in rotor
P	steady static pressure
$\tilde{P}$	first harmonic unsteady pressure

P_∞	steady static pressure far upstream
$r_G = \sqrt{\frac{I}{mb^2}}$	blade section radius of gyration about elastic axis
$S_\alpha = x_\alpha mb$	static mass moment coupling term
s	root locus eigenvalue (Eq. (6)), also cascade gap
t	time
U	rotor blade velocity at leading edge
V	fluid absolute velocity at leading edge
W	fluid inlet relative velocity at leading edge
x_α	offset of airfoil elastic axis from center of gravity nondimensionalized by blade semichord
α	blade torsional displacement about elastic axis
β	cascade stagger angle measured from axial direction
$\delta = \frac{m}{\pi\rho b^2}$	blade/fluid mass ratio
ε	airfoil camber angle, deg
μ	real portion of complex eigenvalue (Eq. (6))
ν	imaginary portion of complex eigenvalue (Eq. (6))
ρ	fluid mass density
σ	interblade phase angle, deg
ω	oscillation frequency, rad/sec, also complex eigenvalue
$\omega_h = \sqrt{\frac{K_h}{m}}$	natural frequency of blade bending motion
$\omega_\alpha = \sqrt{\frac{K_\alpha}{m}}$	natural frequency of blade torsional motion

INTRODUCTION

It is well known that airfoil geometry and steady loading has a strong influence on the unsteady aerodynamic response of cascades. So as the design of modern turbomachinery becomes more stringent to meet specific fatigue and life requirements, the design/analysis for aeroelastic problems will also become more important. It is popularly believed that the modeling of shaped airfoils as unloaded flat plates results in conservative estimates of flutter prediction. The development of an aeroelastic model which accounts for blade thickness, camber, and flow incidence effects is required to determine if this belief is correct and to identify the conditions where it may fail.

The axial-flow turbomachinery blade designer often attempts to model dynamic aeroelastic instabilities through the use of simplified structural and aerodynamic models. Blade-row flutter analyses (Kaza and Kielb, 1982, Kielb and Kaza, 1983, and Srinivasan and Fabunmi, 1975) often employ flat plate, small-disturbance theory (Smith, 1972, and Adamczyk and Goldstein, 1978) to model the unsteady aerodynamic forces acting on vibrating blades. These small-disturbance theories do not account for the effect of airfoil thickness, camber and flow incidence on the unsteady aerodynamic/response of the cascade.

Accounting for airfoil shape and steady loading requires that a more accurate aerodynamic analysis be done. Verdon and Caspar (1982, 1984) have developed an unsteady aerodynamic theory based on a linearization of the unsteady full potential equation. Their method accounts for the effects of blade geometry (i.e., thickness, camber) and steady loading (i.e., flow incidence) on the unsteady potential field within the cascade. Results presented by Verdon (1987) imply that the unsteady aerodynamic response of the cascade is strongly dependent upon the steady flow field which the blade vibrates within. An alternative method for solving the same equation set on practical airfoil geometries has been reported by Whitehead (1982). This technique solves the linearized unsteady potential equation discretized using the finite element method.

The purpose of the current work is to present an aeroelastic analysis scheme which utilizes an unsteady aerodynamic formulation to account for the mentioned steady aerodynamic loading effect on the cascade unsteady aerodynamic behavior. The objective is to study the effect of airfoil shape and steady aerodynamic loading on the tuned flutter characteristics of the cascade. An advantage of this method is that the use of the linearized aerodynamic theory permits the effect of variations in aerodynamic and aeroelastic conditions on flutter characteristics to be examined at reasonable computational cost.

The approach utilizes a two degree-of-freedom (DOF) structural dynamic model of the blade and two-dimensional linearized unsteady potential theory to model the fluid within the cascade. This analysis is presented for a cascade of blades which are representative of compressor blading. The effect of changes in airfoil shape and steady flow incidence are studied to assess their associated impact on the cascade flutter stability.

ANALYTICAL DEVELOPMENT

Aeroelastic Formulation

The model of the turbomachinery blading in this study follows a "typical section" approach wherein the blade is modeled as a rigid airfoil having two DOF. This model assumes the airfoil motion at a representative spanwise location is made up of a bending motion (h) normal to the blade chord and a torsional motion (α) about the elastic axis of the airfoil. Positive directions for these DOF and the resulting forces are indicated in Fig. 1. A full development of the following equations of motion can be found in Bendikson and Friedman (1980).

The dynamic equations of motion for this two DOF blade model are shown below.

$$\begin{bmatrix} m & S_\alpha \\ S_\alpha & I \end{bmatrix} \begin{Bmatrix} \ddot{h} \\ \ddot{\alpha} \end{Bmatrix} + \begin{bmatrix} K_h & 0 \\ 0 & K_\alpha \end{bmatrix} \begin{Bmatrix} h \\ \alpha \end{Bmatrix} = \begin{Bmatrix} L \\ M \end{Bmatrix} \qquad (1)$$

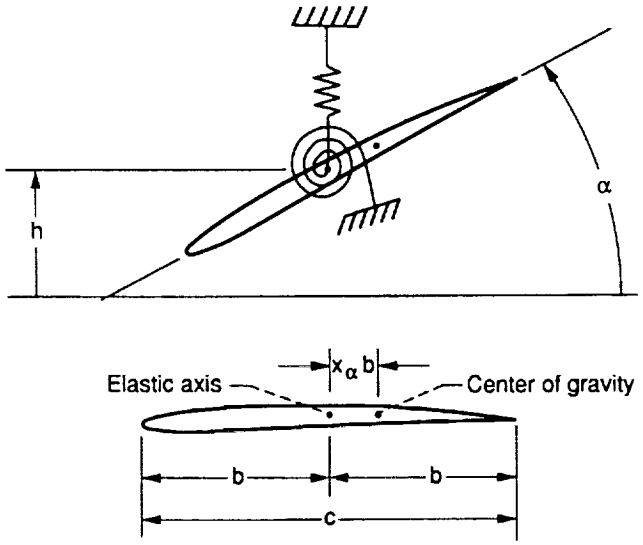

Figure 1.—Typical section airfoil degrees-of-freedom.

The airfoil section mass and moment of inertia are m and I, and lumped springs of stiffness K_h and K_α act at the elastic axis. Inertial coupling may be present due to an offset in the elastic axis from the airfoil center of gravity, and is modeled as a static mass unbalance S_α. The forcing term on the right-hand side of Eq. (1) represents the unsteady aerodynamic forces and moments present during airfoil oscillation.

The vibration of the blade is assumed to occur as small-amplitude and simple harmonic in time, such that the blade displacement vector is

$$\begin{Bmatrix} h \\ \alpha \end{Bmatrix} = \begin{Bmatrix} h_o \\ \alpha_o \end{Bmatrix} e^{i\omega t} \tag{2}$$

The motion-dependent unsteady aerodynamic loads are modeled as first-order harmonic in time as shown in Eq. (3).

$$L = \rho W^2 c \left(L_h \frac{h_o}{c} + L_\alpha \alpha_o \right) e^{i\omega t}$$

$$M = \rho W^2 c^2 \left(M_h \frac{h_o}{c} + M_\alpha \alpha_o \right) e^{i\omega t} \tag{3}$$

The unsteady aerodynamic coefficients L_h, L_α, M_h, M_α are complex quantities which relate the aerodynamic forces and their phase to the corresponding driving motion. For a fixed cascade geometry, these coefficients are strongly dependent upon the cascade operating parameters, relative Mach number M_R, incidence angle i, and the aeroelastic parameters, reduced frequency k and interblade phase angle σ.

Substitution of Eqs. (2) and (3) into Eq. (1) results in an aeroelastic equation which describes the blade/fluid system dynamics. This equation is nondimensionalized by using the nondimensional parameters δ, x_α, r_G, and k. The bending DOF h is also nondimensionalized by the blade chord c and the frequency is normalized by the torsional natural frequency ω_α. The nondimensional flutter equation which results is included below as Eq. (4).

$$\left(\frac{\omega}{\omega_\alpha}\right)^2 \left(\begin{bmatrix} 1 & \frac{X_\alpha}{2} \\ \frac{2X_\alpha}{r_G^2} & 1 \end{bmatrix} + \frac{1}{\delta \pi k^2} \begin{bmatrix} L_h & L_\alpha \\ \frac{4M_h}{r_G^2} & \frac{4M_\alpha}{r_G^2} \end{bmatrix} \right) \begin{Bmatrix} \frac{h_o}{c} \\ \alpha_o \end{Bmatrix} = - \begin{bmatrix} \left(\frac{\omega_h}{\omega_\alpha}\right)^2 & 0 \\ 0 & 1 \end{bmatrix} \begin{Bmatrix} \frac{h_o}{c} \\ \alpha_o \end{Bmatrix} \tag{4}$$

This equation indicates that when using a frequency domain (harmonic) approximation for the blade motion and aerodynamic forces, the motion-dependent forces appear as an "apparent inertia" term in the equations of motion.

The compressor rotor within this work is assumed to be represented by an unwrapped infinite two-dimensional cascade of airfoils. The cascade for this analysis is assumed to vibrate as a "tuned" rotor. A tuned rotor consists of identical blades, with each blade having the same in-vacuum natural frequencies and mode shapes. Such a rotor, when vibrating within a flowing fluid, will have all the blades experiencing the same amplitude of motion, with a constant phase angle between neighboring blades. These phase angles are referred to as "interblade phase angles" and they describe a travelling wave around the periphery of the rotor.

The interblade phase angles are limited to a discrete set of angles as described by Lane (1956) and shown in Eq. (5).

$$\sigma_j = \frac{2\pi(j-1)}{N} \qquad \text{for} \qquad j = 1, \ldots, N \tag{5}$$

This equation implies that a rotor having N blades may vibrate with any one of N possible interblade phase angle modes.

AERODYNAMIC FORMULATION

The aerodynamic forces present on the blade are calculated using the two-dimensional linearized unsteady potential approach of Verdon and Caspar (1984). The unsteady potential flow within the cascade is assumed to be a first-order harmonic perturbation about the nonuniform steady full potential flow. This expansion involves products of both the steady potential and the first-order harmonic potential. Thus, the variations in the steady potential field caused by airfoil shape and flow incidence are coupled to the unsteady flow problem through the governing unsteady field equations.

The approach requires solution of the two-dimensional steady-state full potential equation on a blade-to-blade computational mesh. The method described by Caspar et al. (1983) is used to calculate the steady full potential flow within the blade passages. The unsteady potential flow is then calculated using this steady full potential flow as the mean flow for the cascade.

A complete discussion of this method including some example results may be found in Verdon and Caspar (1984). A comparison of this linearized unsteady potential method with experimental results from two-dimensional oscillating cascades has been reported in Verdon and Usab (1986). A comparison of the unsteady pressures due to torsional vibration of a large-scale compressor rotor has also been reported in Hardin et al. (1987) showing excellent agreement.

FLUTTER SOLUTION

Flutter occurs as a dynamic instability in which the blade motion becomes self-excited by extracting energy from the flowing fluid. This condition may develop when the aerodynamic forces become in-phase with and eventually lead the blade motion. If no other dissipation mechanism exists for the self excitation (e.g., structural damping), the motion will become unstable.

The determination of aeroelastic stability requires the solution of Eq. (4). This equation represents a complex eigenvalue problem which is solved for the eigenvalues ω_1, ω_2. Solution of this second-order equation is accomplished by determining the roots of the quadratic characteristic equation.

The resulting eigenvalues will be complex and they are converted to root locus form by the equation

$$S = i\left(\frac{\omega}{\omega_\alpha}\right) = \mu + i\nu \qquad (6)$$

The real part of this eigenvalue (μ) represents a measure of the aerodynamic damping ratio, and the imaginary part of this eigenvalue (ν) represents the damped natural frequency normalized by the torsional natural frequency. The system will be in a flutter condition when the real part of either eigenvalue (μ_1 or μ_2) becomes equal to or greater than zero. For a tuned rotor, the eigenvalue problem of Eq. (4) is solved N times, for each of the corresponding interblade phase angles of Eq. (5).

The aerodynamic forces are dependent upon several aeroelastic parameters, the most important of which are the reduced frequency k, relative Mach number M_R, and cascade interblade phase angle σ. Therefore, an iterative eigensolution must be used to determine the condition when flutter will occur, i.e., when $\mu = 0$. The flutter iteration for a specified blade geometry and cascade configuration involves prescribing either a Mach number or a reduced frequency, and varying the other parameter while calculating all interblade phase angles for the rotor.

The present method involved specifying a Mach number where a flutter point is desired, and iterating on the reduced frequency until an unstable eigenvalue was obtained for one of the phase angles of the full rotor. An initial guess for the flutter reduced frequency is made and the eigenvalues for all interblade phase angles are calculated. The most unstable eigenvalue (eigenvalue with largest μ) is used to continue in a Newton iteration until convergence.

The algorithm is expressed as

$$k_F^{(n+1)} = k_F^{(n)} - \left(\frac{\Delta k_F}{\Delta \mu}\right)^{(n)} \mu^{(n)} \qquad (7)$$

where n signifies the iteration level, k_F is the flutter reduced frequency and μ is the real portion of the eigenvalue for the most unstable interblade phase angle mode. It has been found that this procedure usually converges within from 4 to 6 iterations.

APPLICATION OF METHOD

Compressor Cascade

The application of this aeroelastic model is presented for a cascade of blades representative of current compressor blade designs. The airfoil shape used for this work is a NACA 0006 series airfoil thickness distribution applied along a circular arc mean camber line. The camber was varied by changing the height of the camber line. The camber angle is represented as ε which is the difference in the inlet metal and exit metal angles at the airfoil leading and trailing edges. An illustration of the compressor cascade denoting the cascade nomenclature is included as Fig. 2. The cascade parameters chosen to represent this compressor cascade are listed in Table I.

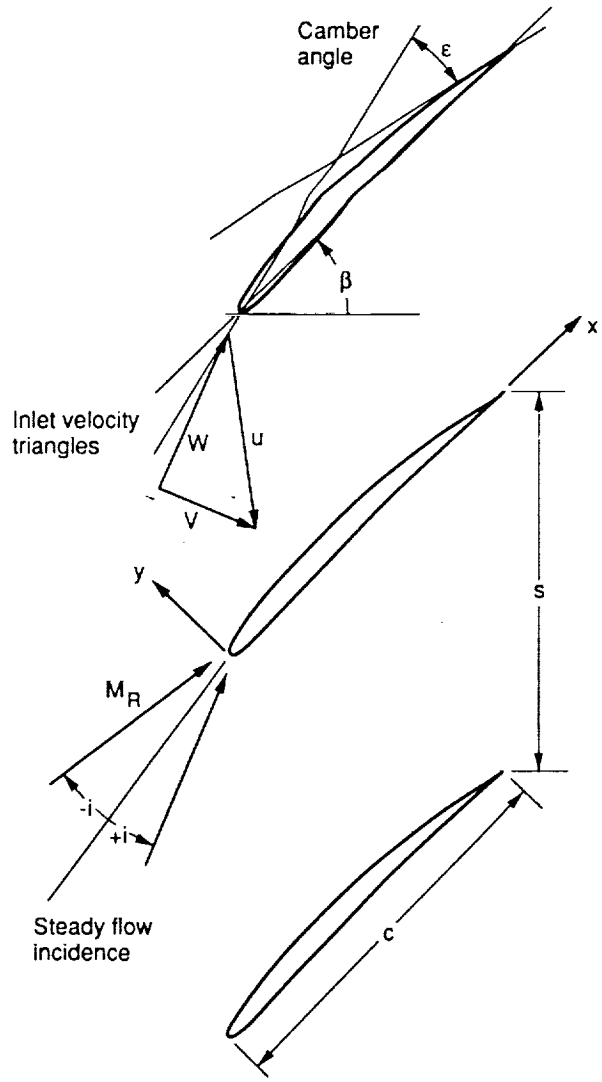

Figure 2.—Cascade geometry and nomenclature.

The airfoil inertial properties were determined using numerical integration to calculate the airfoil center of gravity, moment of inertia, and radius of gyration. A number of airfoils were studied in this work, ranging in camber angles from 0° to 30°. The

TABLE I. - CASCADE DESCRIPTION

Airfoil thickness distribution	NACA 0006
Cascade stagger angle, β, deg	45
Cascade solidity, c/s	1.0
Blade-fluid mass ratio, μ	330
Frequency ratio, ω_h/ω_α	0.30
Radius of gyration, r_G	Varied
E.A. - C.G. offset, x_α	Varied
Number of blades, N	12
Elastic axis location	0.5,0.0

TABLE II. - CAMBERED AIRFOIL INERTIAL PROPERTIES

Camber angle, ε, deg	Center of gravity		r_G	x_α
	x	y		
0	0.4180	0.0000	0.4953	-0.1640
5	.4180	.0083	.4955	-.1640
10	.4179	.0165	.4962	-.1642
15	.4179	.0248	.4981	-.1642
20	.4178	.0331	.5016	-.1644
25	.4177	.0415	.5045	-.1646
30	.4175	.0498	.5088	-.1652

elastic axis for all the airfoils was chosen to be at midchord. The airfoil properties for all of the camber angles studied are included in Table II.

The aeroelastic analyses were conducted to determine the effect of (1) airfoil shape and (2) steady flow incidence on the flutter behavior of a tuned cascade. Flutter was determined by solving the eigenvalue problem of Eq. (4) which not only includes aerodynamic properties of the system, but also the structural dynamic properties. This method of analysis was chosen because it is similar to the type of analysis that a designer may use during initial component design analysis. For all cases, the inlet relative Mach number was limited to subsonic values such that no shocks would appear within the cascade. This was done so that the effect of variations in the mean potential field due to blade shape and incidence could be studied, where there were no flow discontinuities occurring in the potential field.

AERODYNAMIC ANALYSIS

The aerodynamic analysis method employed in this work requires that two-dimensional computational meshes be used to perform the finite-difference solution of the governing equations. The current method uses a blade-to-blade H-type computational mesh to capture the global flow behavior over a single blade passage. A local C-type grid is then required to more accurately resolve the flows around the leading edge region of the blade. An example of these global and local computational meshes is included as Fig. 3 for a cascade having 20° camber angle. A dependence upon local mesh discretization was encountered during the analysis, so the leading edge local mesh was refined until successive flow solutions indicated a convergence to a steady surface pressure distribution about the blade. The meshes used for all the analyses were of size 75×30 for the global mesh and 70×11 for the local mesh.

The steady full potential flow in the cascade was computed using the method described previously. Calculations were performed for Mach numbers up to $M_R = 0.7$. The calculated static pressure coefficient C_p is shown in Fig. 4 for an inlet Mach number of 0.60

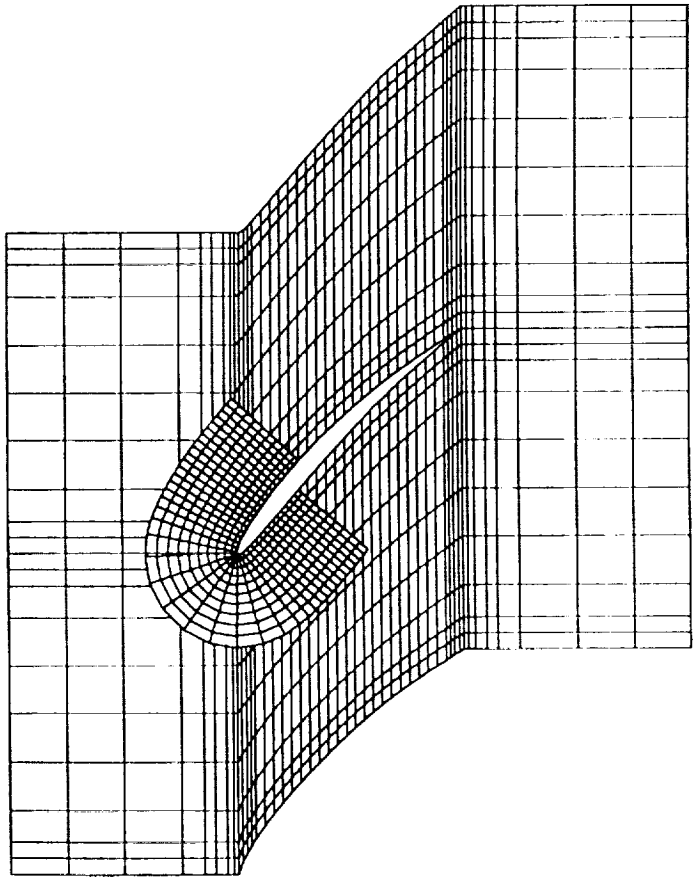

Figure 3.—Unsteady aerodynamic computational meshes.

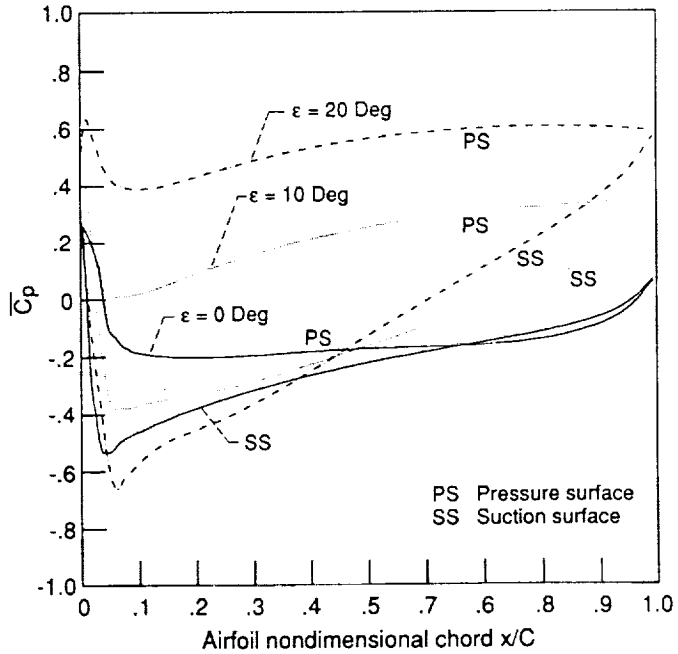

Figure 4.—Steady surface pressure distributions (NACA 0006 airfoils, M = 0.60, i = 0°).

for NACA 0006 airfoils having camber angles of 0°, 10°, and 20°. Calculations were also performed for a NACA 0006 with 10° camber cascade at incidence angles of -4°, 0°, and 4° as shown on Fig. 5. This figure shows

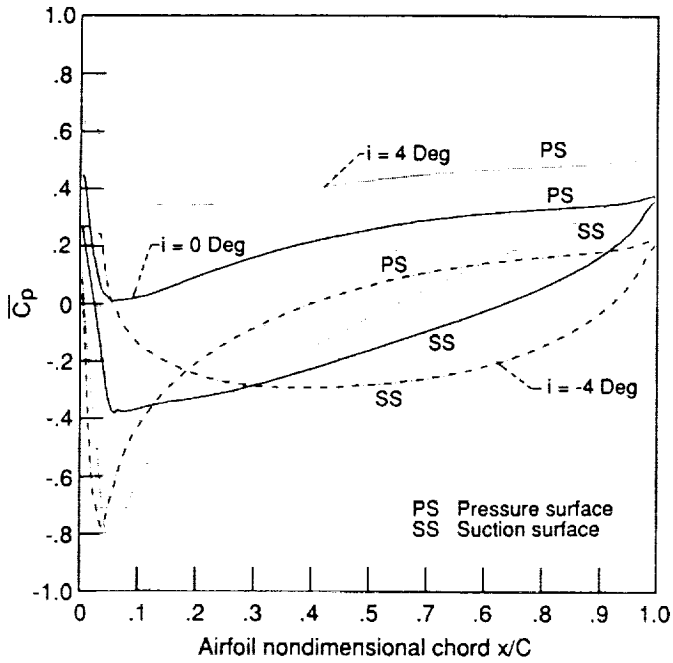

Figure 5.—Steady surface pressure distributions (NACA 0006 airfoils, M = 0.60, ε = 0°).

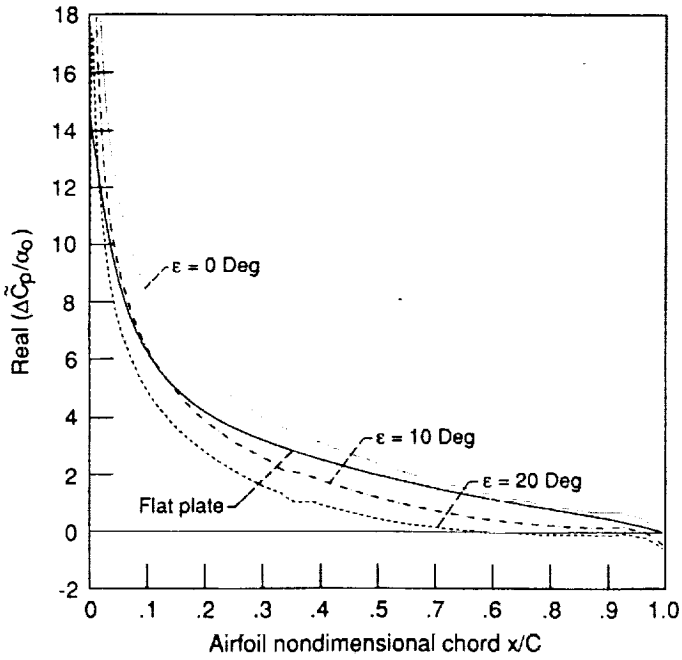

Figure 6.—Unsteady surface pressure distributions - real part (NACA 0006 airfoils, M = 0.60, i = 0°, σ = 60°).

the off-design effects such as the large expansion near the leading edge for the 4° incidence case and the underexpansion which occurs for the -4° case. These conditions may be encountered during partial speed operation of the compressor.

The unsteady pressures due to torsional motion of the airfoil about the elastic axis were calculated for airfoils having camber angles of 0°, 10°, and 20°. The inlet Mach number was 0.60 and the incidence angle for all cases was 0°. The reduced frequency was k = 0.22 and the interblade phase angle was σ = 60°. Plots showing the unsteady surface pressure coefficient difference across the airfoil are shown in Fig. 6 (real part) and Fig. 7 (imaginary part). The results from a flat plate airfoil modeled using the same method are also included for reference. The unsteady pressure coefficient is normalized by the magnitude of the torsional motion.

It is important to observe that two basic effects are present for this unsteady flow problem. There is an influence due to the dependence of the unsteady potential equation on the underlying steady potential

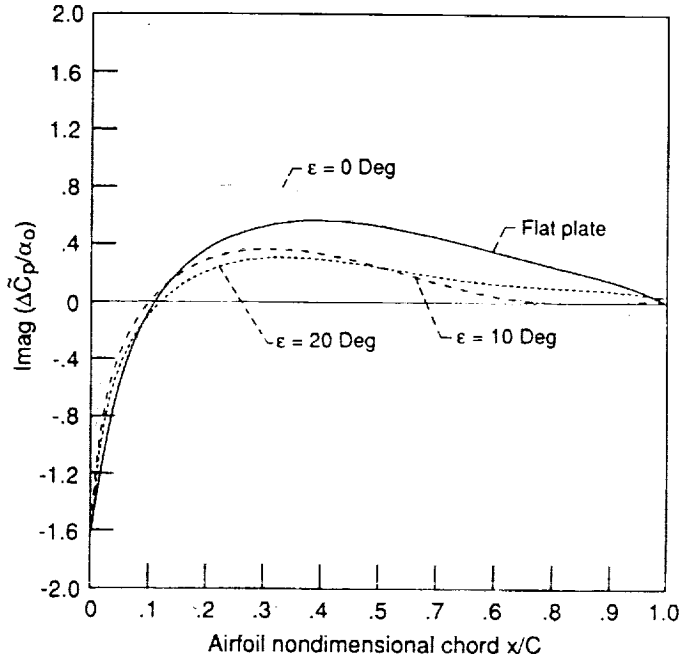

Figure 7.—Unsteady surface pressure distributions - imaginary part (NACA 0006 airfoils, M = 0.60, i = 0°, σ = 60°).

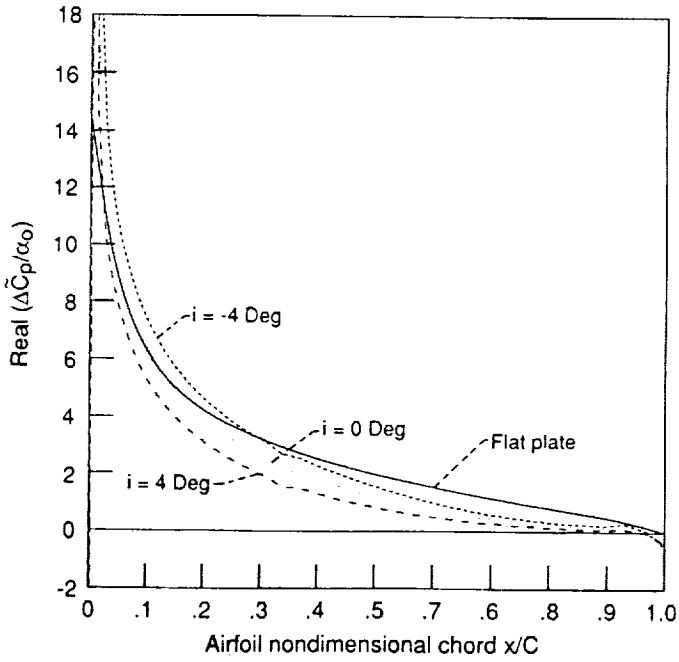

Figure 8.—Unsteady surface pressure distributions - real (NACA 0006 airfoils, M = 0.60, ε = 0°, σ = 60°).

field. In addition, there is also the effect of changes in the airfoil surface boundary condition for airfoils of different camber. A determination of which of these two effect is more important is not obvious based on these results.

Therefore, an analysis was conducted to study the effect of flow incidence (changing steady potential field alone) for the same cambered airfoil under the same operating conditions. Results showing the unsteady pressure difference caused by torsional motion for a 10° cambered airfoil at three different incidence angles are included on Figs. 8 and 9. As before, the reduced frequency was k = 0.22 and the interblade phase angle was 60°. Both positive and negative incidence angles are included to simulate off-design operating conditions. These unsteady pressure results resemble those presented for camber angle changes, although the imaginary pressures seem to depend more strongly upon incidence, particularly in the region from midchord aft to the trailing edge.

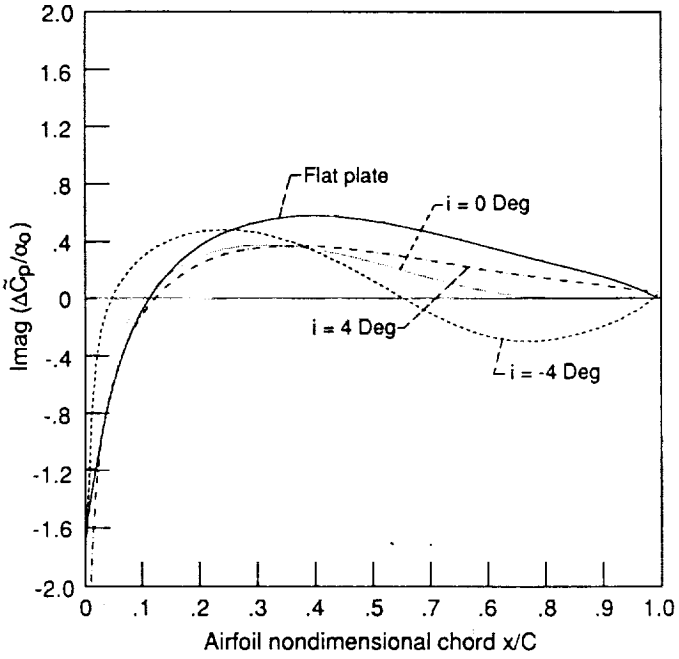

Figure 9.—Unsteady surface pressure distributions - imaginary part (NACA 0006 airfoils, M = 0.60, ε = 10°, σ = 60°).

AEROELASTIC ANALYSIS

The dependence of unsteady surface pressures on the steady aerodynamic loading level has been studied in the previous section. In the current section, an investigation of the same effect on the overall aeroelastic stability is presented. The flutter solution for the cascades was determined by solving Eq. (4) for a range of camber angles and operating Mach numbers. The solution of this tuned aeroelastic eigenvalue problem is required for all interblade phase angles which occur for the rotor, in this case N = 12. The resulting set of complex eigenvalues form the locus of roots, where one root will become most unstable.

This root locus has been calculated for the example rotor operating at a relative Mach number of 0.60 and a reduced frequency of k = 0.22. The four cases analyzed consisted of a flat plate airfoil, and NACA 0006 airfoils having 0°, 10°, and 20° camber. The root

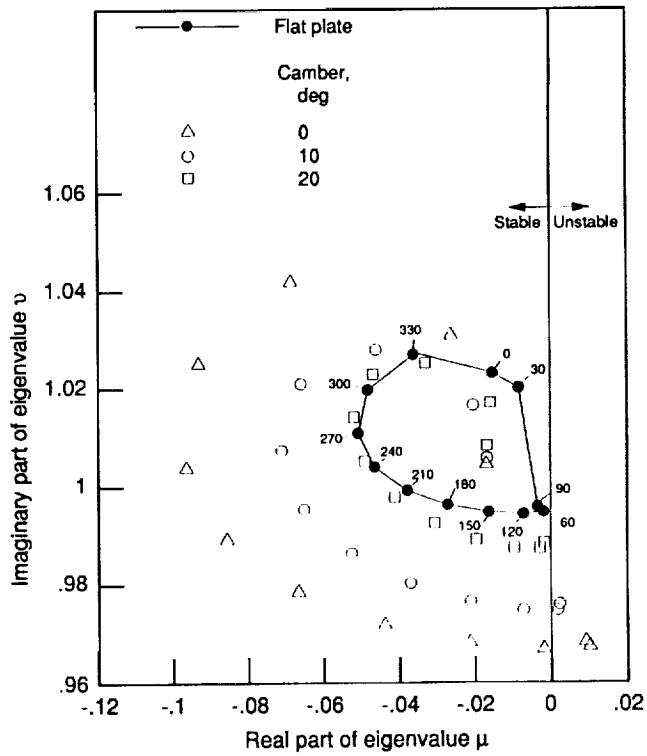

Figure 10.—Tuned rotor root locus showing effect of airfoil camber (torsion mode, M = 0.60, i = 0°, k = 0.22).

locus shown on Fig. 10 shows the four loci corresponding to these cascades, where the eigenvalues corresponding to the torsional DOF are shown, as this was the most unstable mode of vibration. The modes corresponding to bending motion of the blade were always more stable than those corresponding to torsional motion of the blade. The numbers on the plot represent the interblade phase angle modes for the tuned rotor. These calculations show a large difference between the flat plate airfoil and the 0° camber airfoil rotors, where the only difference is due to the airfoil thickness distribution. The rotor of uncambered airfoils is the most unstable, with increasing airfoil camber causing the rotor to become more stable.

The above result implies that the modeling of a low cambered compressor under the assumption that a flat plate aerodynamic representation is valid may not always be as conservative as is often assumed. Additionally, the effect of increasing airfoil camber appears to cause the rotor to become more stable. In fact, these results imply that the flat plate results always underpredict the flutter condition when compared to the results when airfoil shape and flow incidence are considered.

A similar calculation was performed to determine the root locus for the NACA 0006 10° camber airfoil at incidence angles of -4°, 0°, and 4°. As before, the relative Mach number was 0.6 and the reduced frequency k = 0.22. The root loci are shown on Fig. 11 for the flat plate cascade and the 10° camber airfoil at negative and positive incidence levels. These calculations were performed to determine the effect of off-design conditions due to inlet flow angle variations on the rotor stability. These results indicate that positive flow incidence makes the rotor become more stable when

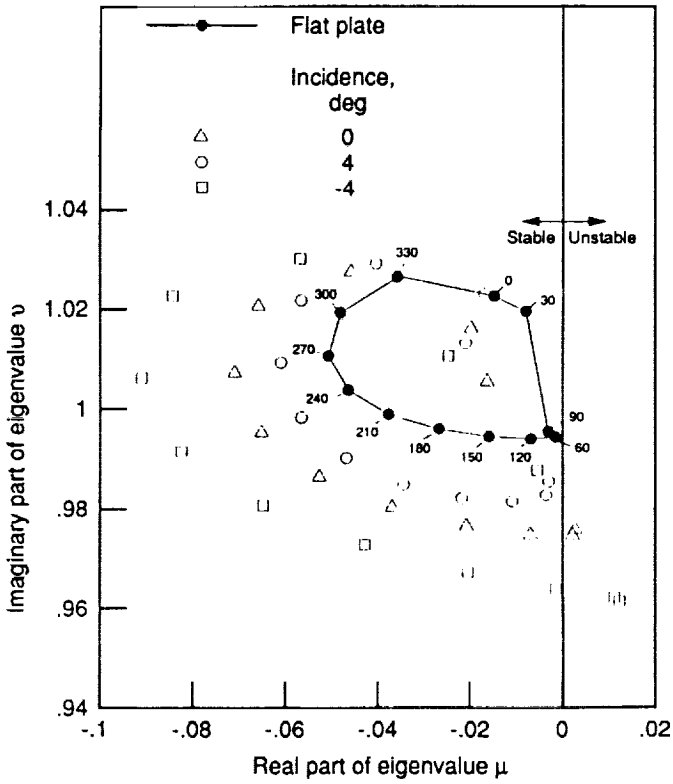

Figure 11.—Tuned rotor root locus showing effect of flow incidence (NACA 0006 airfoil, ε = 10°, torsion mode, M = 0.60, k = 0.22).

compared to zero incidence. Likewise, negative incidence causes a strong destabilization of the rotor, as shown by the large spread of the -4° incidence eigenvalues relative to the zero incidence case. Obviously none of these characteristics would be identified using flat plate small-disturbance aerodynamic theories.

FLUTTER ANALYSIS

The aeroelastic stability analysis for the rotor was studied in order to determine the effect of airfoil camber and flow incidence on the flutter behavior. The iterative flutter search method was implemented in order to perform the flutter analysis more efficiently. The effect of parametric changes in airfoil camber angle on the flutter boundary for a tuned rotor operating at inlet Mach numbers of 0.5 to 0.7 was studied. Figure 12 shows the flutter boundaries for these operating conditions where the fluttering mode was a torsional mode in all cases. Note the apparent linearity of the flutter reduced frequency with increasing airfoil camber. The flutter reduced frequencies for the flat plate are also shown on this figure as symbols. Note that the flat plate results are constant with changes in camber angle.

The effect of variations in the mean flow incidence angle on the flutter characteristics was also determined. The flutter boundaries for the tuned rotor operating at a Mach number of 0.6 is shown on Fig. 13 as a function of positive and negative mean flow incidence angles. This figure includes the results for the NACA 0006 airfoils having camber angles of 0°, 10° and 20°. Additionally, the flat plate flutter point is also shown on this figure as a point. Usually, the designer considers a lower flutter reduced frequency as better, because it permits higher relative

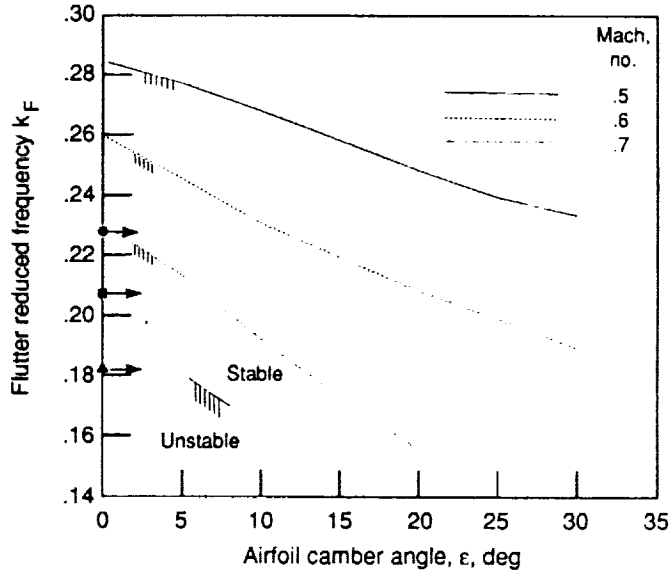

Figure 12.—Effect of airfoil camber angle on flutter boundary (NACA 0006 airfoils, torsion mode, i = 0°). Symbols denote flat plate results.

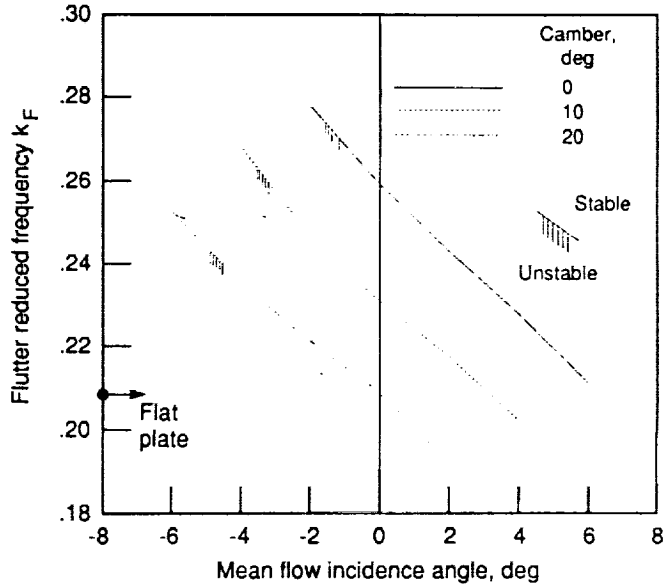

Figure 13.—Effect of mean flow incidence on flutter boundary (NACA airfoils, torsion mode, M = 0.60).

fluid velocities. This figure indicates that operating at off-design negative incidence angles (engine deceleration, approaching choking) can have an undesirable effect on the rotor stability. These calculations were performed using inviscid potential flow theory, and the authors realize the limitations of inviscid flow models when applied to flows at high incidence angles.

COMPUTER TIME

The use of the linearized unsteady aerodynamic theory presents a significant advantage over other recent unsteady CFD methods because of its rapid computational time. The current implementation computes one set of unsteady aerodynamic coefficients (i.e., L_h and M_h) in about 8 CPU seconds on the NASA Lewis Cray X-MP computer. The calculation of a full tuned rotor root

locus required approximately 180 CPU seconds. The iterative flutter solution for one Mach number and incidence angle required approximately 1600 CPU seconds. These figures represent a cost advantage of more than an order of magnitude reduction in CPU time when compared to other recently proposed CFD methods.

CONCLUSIONS

A numerical study of the influence of steady aerodynamic loading on the flutter behavior of a tuned compressor rotor was performed. The results of this analysis imply the following:

1. Airfoil camber and thickness has a strong influence on the unsteady surface pressures induced by airfoil oscillation.
2. The effect of steady flow incidence on the unsteady surface pressures can be as strong or stronger than the effect of airfoil camber alone.
3. The impact of steady aerodynamic loading caused by airfoil camber, thickness and flow incidence, is significant with respect to rotor flutter calculations when compared to a traditional flat-plate aerodynamic analysis.
4. Unloaded flat plate results indicated a strong difference from the analyses which accounted for airfoil shape, implying that the flat plate assumption would not properly predict the occurrence of flutter.
5. The presented results indicate that the effect of airfoil camber angle and steady flow incidence shows a fairly linear behavior with respect to flutter boundaries within the range of parameters which may be considered during the design process.

The intent of this work was not to present a complete flutter analysis for a specific class of turbomachinery. The objective was to demonstrate the effect of some practical design parameters on the overall aeroelastic stability of rotors. The continued development of state-of-the-art unsteady aerodynamic models for turbomachinery flows is making the task of aeroelastic analysis of real-world blading more practical.

ACKNOWLEDGMENTS

This work was supported under NASA contract number NAS3-25266, George Stefko and Oral Mehmed, technical monitors.

REFERENCES

Adamczyk, J.J., and Goldstein, M.E., 1978, "Unsteady Flow in a Supersonic Cascade with Subsonic Leading-Edge Locus," AIAA Journal, Vol. 16, pp. 1248-1254.

Bendiksen, O., and Friedmann, P., 1980, "Coupled Bending-Torsion Flutter in Cascades," AIAA Journal, Vol. 18, pp. 194-201.

Caspar, J.R., 1983, "Unconditionally Stable Calculation of Transonic Potential Flow Through Cascades Using an Adaptive Mesh for Shock Capture," Journal of Engineering for Power, Vol. 105, pp. 504-513.

Hardin, L.W., Carta, F.O., and Verdon, J.M., 1987, "Unsteady Aerodynamic Measurements on a Rotating Compressor Blade Row at Low Mach Numbers," ASME Paper 87-GT-221.

Kaza, K.R.V., and Kielb, R. E., 1982, "Flutter and Response of a Mistuned Cascade in Incompressible Flow," AIAA Journal, Vol. 20, pp. 1120-1127.

Kielb, R.E., and Kaza, K.R.V., 1983, "Aeroelastic Characteristics of a Cascade of Mistuned Blades in Subsonic and Supersonic Flows," Journal of Vibration, Acoustics, Stress, and Reliability in Design, Vol. 105, pp. 425-433.

Lane, F., 1956, "System Mode Shapes in the Flutter of Compressor Blade Rows," Journal of the Aeronautical Sciences, Vol. 23, pp. 54-66.

Smith, S.N., 1972, "Discrete Frequency Sound Generation in Axial Flow Turbomachines," Aeronautical Research Council, ARC-R/M-3709.

Srinivasan, A.V., and Fabunmi, J.A., 1984, "Cascade Flutter Analysis of Cantilevered Blades," Journal of Engineering for Gas Turbines and Power, Vol. 106, pp. 34-43.

Verdon, J.M., and Caspar, J.R., 1982, "Development of a Linear Unsteady Aerodynamic Analysis for Finite-Deflection Subsonic Cascades," AIAA Journal, Vol. 20, pp. 1259-1267. (Also, AIAA Paper 81-1290, June 1981).

Verdon, J.M, and Caspar, J.R., 1984, "A Linearized Unsteady Aerodynamic Analysis for Transonic Cascades," Journal of Fluid Mechanics, Vol. 149, pp. 403-429.

Verdon, J.M., and Usab, W.J., 1986, "Application of a Linearized Unsteady Aerodynamic Analysis to Standard Cascade Configurations," NASA CR-3940.

Verdon, J.M., 1987, "The Unsteady Aerodynamic Response to Arbitrary Modes of Blade Motion," Unsteady Aerodynamics and Aeroelasticity of Turbomachines and Propellers, Proceedings of the Fourth International Symposium, Aachen, West Germany, Sept. 6-10, 1987, Rheinsch-Westfallische Technische Hochschule Aachen, pp. 313-334.

Whitehead, D.S., 1982, "The Calculation of Steady and Unsteady Transonic Flow in cascades," Cambridge University Engineering Department, Report CUED/A-Turbo/TR 118.

NASA
National Aeronautics and Space Administration

Report Documentation Page

1. Report No.	2. Government Accession No.	3. Recipient's Catalog No.
NASA CR-187055		

4. Title and Subtitle	5. Report Date
The Effect of Steady Aerodynamic Loading on the Flutter Stability of Turbomachinery Blading	December 1990
	6. Performing Organization Code

7. Author(s)	8. Performing Organization Report No.
Todd E. Smith and Jaikrishnan R. Kadambi	None (E-5929)
	10. Work Unit No. 590-21-31

9. Performing Organization Name and Address	11. Contract or Grant No.
Sverdrup Technology, Inc. Lewis Research Center Group 2001 Aerospace Parkway Brook Park, Ohio 44142	NAS3-25266
	13. Type of Report and Period Covered Contractor Report Final
12. Sponsoring Agency Name and Address	14. Sponsoring Agency Code
National Aeronautics and Space Administration Lewis Research Center Cleveland, Ohio 44135-3191	

15. Supplementary Notes

Project Manager, George L. Stefko, Structures Division, NASA Lewis Research Center. Prepared for the 36th International Gas Turbine and Aeroengine Congress and Exposition, sponsored by the American Society of Mechanical Engineers, Orlando, Florida, June 3-6, 1991. Todd E. Smith, Sverdrup Technology, Inc., Lewis Research Center Group, 2001 Aerospace Parkway, Brook Park, Ohio 44142; Jakrishnan R. Kadambi, Department of Mechanical and Aerospace Engineering, Case Western Reserve University, Cleveland, Ohio 44106.

16. Abstract

An aeroelastic analysis is presented which accounts for the effect of steady aerodynamic loading on the aeroelastic stability of a cascade of compressor blades. The aeroelastic model is a two degree-of-freedom model having bending and torsional displacements. A linearized unsteady potential flow theory is used to determine the unsteady aerodynamic response coefficients for the aeroelastic analysis. The steady aerodynamic loading was caused by the addition of (a) airfoil thickness and camber and (b) steady flow incidence. The importance of steady loading on the airfoil unsteady pressure distribution is demonstrated. Additionally, the effect of the steady loading on the tuned flutter behavior and flutter boundaries indicates that neglecting either airfoil thickness, camber or incidence could result in nonconservative estimates of flutter behavior.

17. Key Words (Suggested by Author(s))	18. Distribution Statement
Aeroelasticity Flutter Turbomachinery blading	Unclassified – Unlimited Subject Category 39

19. Security Classif. (of this report)	20. Security Classif. (of this page)	21. No. of pages	22. Price*
Unclassified	Unclassified	10	A02

*For sale by the National Technical Information Service, Springfield, Virginia 22161